# Epidermis-Intrinsic Transcription Factor Ovol1 Coordinately Regulates Barrier Maintenance and Neutrophil Accumulation in Psoriasis-Like Inflammation



Morgan Dragan<sup>1,2,3,8</sup>, Peng Sun<sup>1,8</sup>, Zeyu Chen<sup>1,4,5</sup>, Xianghui Ma<sup>1</sup>, Remy Vu<sup>1,2</sup>, Yuling Shi<sup>5,6</sup>, S. Armando Villalta<sup>3,7</sup> and Xing Dai<sup>1,2,3</sup>

Skin epidermis constitutes the exterior barrier that protects the body from dehydration and environmental assaults. Barrier defects underlie common inflammatory skin diseases, but the molecular mechanisms that maintain barrier integrity and regulate epidermal—immune cell cross-talk in inflamed skin are not fully understood. In this study, we show that skin epithelia-specific deletion of *Ovol1*, which encodes a skin disease—linked transcriptional repressor, impairs the epidermal barrier and aggravates psoriasis-like skin inflammation in mice in part by enhancing neutrophil accumulation and abscess formation. Through molecular studies, we identify IL-33, a cytokine with known pro-inflammatory and anti-inflammatory activities, and Cxcl1, a neutrophil-attracting chemokine, as potential weak and strong direct targets of Ovol1, respectively. Furthermore, we provide functional evidence that elevated *Il33* expression reduces disease severity in imiquimod-treated *Ovol1*-deficient mice, whereas persistent accumulation and epidermal migration of neutrophils exacerbate it. Collectively, our study uncovers the importance of an epidermally expressed transcription factor that regulates both the integrity of the epidermal barrier and the behavior of neutrophils in psoriasis-like inflammation.

Journal of Investigative Dermatology (2022) 142, 583-593; doi:10.1016/j.jid.2021.08.397

### **INTRODUCTION**

Skin epidermis is a self-renewing epithelium composed of stem/progenitor cells that terminally differentiate to produce stratum corneum, which constitutes a physical barrier at the skin's outmost surface against myriad external assaults (Gonzales and Fuchs, 2017). Common inflammatory skin diseases such as psoriasis and atopic dermatitis are associated with disruption of this epidermal barrier either as a trigger for disease or as a secondary consequence of immune cell dysregulation (Harden et al., 2015; Ring et al., 2012; Schmuth et al., 2015; Segre, 2006). Moreover,

<sup>1</sup>Department of Biological Chemistry, School of Medicine, University of California, Irvine, Irvine, California, USA; <sup>2</sup>NSF-Simons Center for Multiscale Cell Fate Research, University of California, Irvine, Irvine, California, USA; <sup>3</sup>Institute for Immunology, University of California, Irvine, Irvine, California, USA; <sup>4</sup>Department of Dermatology, Shanghai Tenth People's Hospital, School of Medicine, Tongji University, Shanghai, China; <sup>5</sup>Institute of Psoriasis, School of Medicine, Tongji University, Shanghai, China; <sup>6</sup>Department of Dermatology, Shanghai Skin Disease Hospital, School of Medicine, Tongji University, Shanghai, China; and <sup>7</sup>Department of Physiology & Biophysics, School of Medicine, University of California, Irvine, Irvine, California, USA

<sup>8</sup>These authors contributed equally to this work.

Correspondence: Xing Dai, Department of Biological Chemistry, School of Medicine, University of California, Irvine, D250 Medical Sciences I, Irvine, California 92697-1700, USA. E-mail: xdai@uci.edu

Abbreviations: IMQ, imiquimod; KC, keratinocyte; SSKO, skin epithelia–specific knockout; TEWL, transepidermal water loss; Treg, regulatory T cell Received 13 May 2021; revised 22 July 2021; accepted 13 August 2021; accepted manuscript published online 27 August 2021; corrected proof published online 5 October 2021

disease progression is facilitated by epidermal cell regulation of and response to immune cells (Kobayashi et al., 2019; Pasparakis et al., 2014; Zhang et al., 2019). However, the molecular mechanisms that regulate epidermally driven communication between epidermal and immune cells in coordination with barrier maintenance remain largely unknown.

Previously, we reported that germline deletion of Ovol1, which encodes a transcription factor known to regulate epidermal development (Dai et al., 1998; Lee et al., 2014; Nair et al., 2006; Teng et al., 2007), leads to exacerbated skin inflammation and epidermal hyperplasia in response to imiquimod (IMQ), an agent widely used to induce psoriasislike symptoms in mice (Sun et al., 2021; van der Fits et al., 2009). Moreover, human *OVOL1* is upregulated in psoriatic lesions (Sun et al., 2021). Neutrophil accumulation in differentiated layers of the epidermis (Munro's abscesses) distinguishes a subset of human patients with psoriasis and is a key feature of psoriasis-like skin inflammation in mice (Chiang et al., 2019; Pinkus and Mehregan, 1966; Sumida et al., 2014; Uribe-Herranz et al., 2013). Epidermal keratinocytes (KCs) play an important role in neutrophil recruitment by secreting cytokine/chemokines such as IL-1α, CXCL1, CXCL8, and LTB<sub>4</sub> (Milora et al., 2015; Olaru and Jensen, 2010; Sumida et al., 2014; Sun et al., 2021). Although we found elevated levels of IL-1 $\alpha$  in IMQ-treated Ovol1 null epidermis (Sun et al., 2021), it remains unclear whether Ovol1 functions within the epidermis to directly regulate epidermal neutrophil cross-talk and whether it promotes barrier integrity.

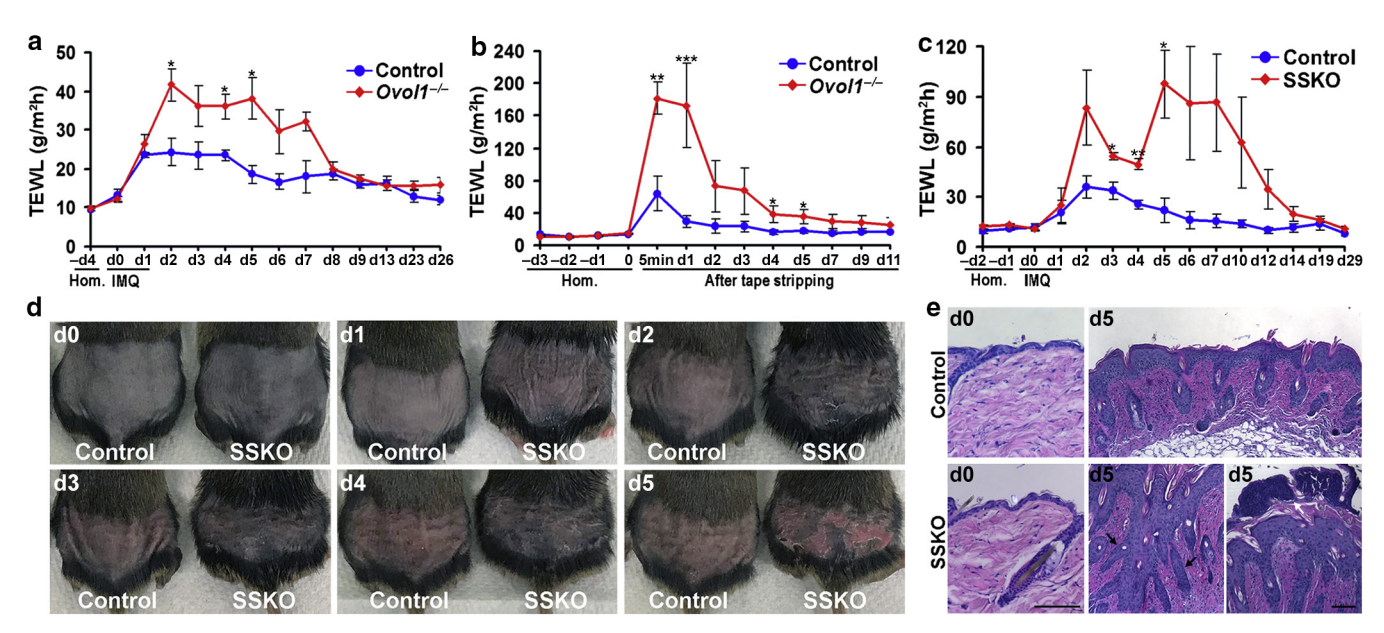


Figure 1. Loss of *Ovol1* in the epidermis aggravates IMQ-induced barrier disruption and epidermal hyperplasia. ( $\mathbf{a}-\mathbf{c}$ ) TEWL measurements of ( $\mathbf{a}$ ,  $\mathbf{b}$ )  $Ovol1^{-/-}$  or ( $\mathbf{c}$ ) Ovol1 SSKO mice along with their control littermates after ( $\mathbf{a}$ ,  $\mathbf{c}$ ) IMQ treatment or ( $\mathbf{b}$ ) tape stripping, starting on d0, where d before perturbation represent Hom.  $\mathbf{n}=3$  for control littermates in  $\mathbf{a}-\mathbf{c}$ . For mutants, ( $\mathbf{a}$ )  $\mathbf{n}=5$  ( $\mathbf{b}$ ,  $\mathbf{c}$ )  $\mathbf{n}=3$ . ( $\mathbf{d}$ ) External appearance at different d after the first IMQ application. ( $\mathbf{e}$ ) Skin histology on d0 and d5. Black and white arrows point to finger-like epidermal projections and neutrophil aggregates on the skin surface, respectively. Bar = 100  $\mu$ m. \*\*\* P < 0.005; \*\* P < 0.01; \* P < 0.05. Error bars represent mean  $\pm$  SEM. d, day; Hom, homeostasis; IMQ, imiquimod; SSKO, skin epithelia—specific knockout; TEWL, transepidermal water loss.

In this work, we generated and analyzed mice with skin epithelia-specific knockout (SSKO) of Ovol1 and examined their responses to IMQ. We found that epidermal loss of Ovol1 dramatically aggravates IMQ-induced barrier disruption, epidermal hyperplasia, and neutrophil accumulation. In contrast, there was a reduction of lymphocytes, except for regulatory T cells (Tregs). We detected upregulated expression of 1/33—the human counterpart of which is suppressed by OVOL1 overexpression (Furue et al., 2019; Tsuji et al., 2020)—in the skin of Ovol1 SSKO mice but found IL-33 antibody neutralization to further enhance the psoriasis-like skin phenotypes of these mice. We showed that Ovol1 protein binds weakly to the 1/33 promoter but strongly to the promoter of Cxcl1, and indeed Cxcl1 expression was elevated in Ovol1-deficient epidermis. Finally, we obtained evidence that Ovol1 loss facilitates neutrophil accumulation near and migration through the epidermis and that neutrophil depletion partially mitigates the psoriasis-like phenotypes of Ovol1-deficient mice. Together, our findings uncover an epidermal-intrinsic transcription factor that both promotes barrier integrity and directly suppresses neutrophil accumulation in psoriasis-like inflammation.

### **RESULTS**

# Ovol1 acts in the epidermis to promote robust barrier maintenance and to suppress IMQ-induced epidermal hyperplasia

The skin of *Ovol1*<sup>-/-</sup> mice exhibit elevated *II1a* expression in response to IMQ (Sun et al., 2021). Because barrier disruption increases *II1a* transcription (Wood et al., 1992), we asked whether *Ovol1*<sup>-/-</sup> skin is barrier defective by performing transepidermal water loss (TEWL) measurements, a widely used method to assess epidermal barrier function (Alexander et al., 2018). During homeostasis (day 0), TEWL values were

the same between *Ovol1*<sup>-/-</sup> and control littermates (Figure 1a and b). However, after IMQ treatment, which is known to induce transient barrier disruption (Barland et al., 2004), the *Ovol1*<sup>-/-</sup> mutants displayed significantly higher and longerlasting TEWL increases than their control littermates (Figure 1a). Similarly, enhanced barrier disruption was observed in *Ovol1*<sup>-/-</sup> mice after tape stripping (Figure 1b).

To ask whether *Ovol1* functions within the epidermis to regulate barrier maintenance, we generated *Ovol1* SSKO (*Ovol1*<sup>-/f</sup>; *K14-Cre*, where *Ovol1* is deleted in epithelial cells of the skin) mice in a congenic C57BL/6 (B6) background. Similar to *Ovol1*<sup>-/-</sup> mice, during homeostasis, TEWL values in *Ovol1* SSKO mice showed no deviation from those of their control littermates (Figure 1c). Consistently, expression of epidermal terminal differentiation markers appeared largely normal in *Ovol1* SSKO skin (Supplementary Figure S1a). On IMQ treatment, *Ovol1* SSKO mice displayed significantly more dramatic and persistent TEWL increases than their control littermates (Figure 1c). Therefore, *Ovol1* expression in the epidermis is required for maintaining a robust barrier when skin is under external physical or chemical assaults.

We also asked whether *Ovol1* suppression of IMQ-induced inflammation is intrinsic to the epidermis. *Ovol1* SSKO mice showed dramatically more severe psoriasis-like phenotypes that included erythema, scaling, and epidermal hyperplasia after 5 consecutive days of IMQ treatments than weight- and sex-matched littermate controls (Figure 1d and e). Exacerbated phenotypes of *Ovol1* SSKO mice could also be observed after only 2 consecutive days of IMQ treatments (Supplementary Figure S1b). Interestingly, under identical IMQ treatment conditions, the psoriatic-like symptoms, including epidermal hyperplasia, of *Ovol1* SSKO mice appeared comparable with, if not more remarkable than, those of the *Ovol1*<sup>-/-</sup> mice, with the SSKO skin presenting

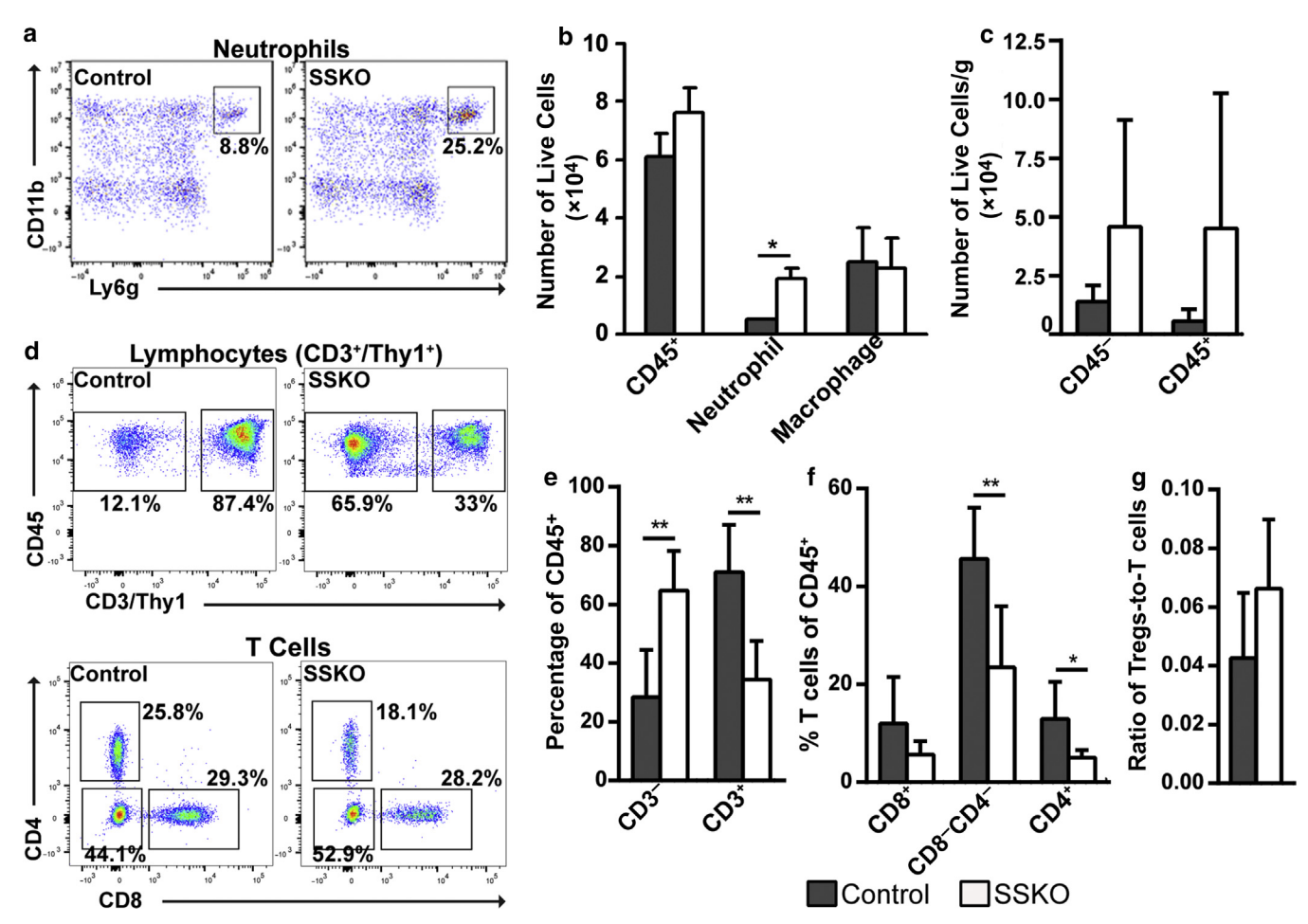


Figure 2. Immune cell profiles in IMQ-treated control and *Ovol1* SSKO skin. Shown are summaries of the flow cytometry data collected (a) 24 hours and (b—e) 6d after the second IMQ application. Representative flow plots are shown in Supplementary Figure S2. (a) n = 3 pairs of *Ovol1* SSKO and control littermates and (b—e) n = 7 control and n = 6 mutants. \*\* P < 0.01; \* P < 0.05. Error bars represent mean  $\pm$  SD. IMQ, imiquimod; SSKO, skin epithelia—specific knockout; Treg, regulatory T cell.

finger-like projections reminiscent of the elongated rete ridges in psoriasiform hyperplasia of human patients (Murphy et al., 2007) (Figure 1e and Supplementary Figure S1c and d). Together, our findings show that *Ovol1* is required in the epidermis to suppress IMQ-induced epidermal hyperplasia and the associated skin phenotypes.

# Acute immune responses in IMQ-treated *Ovol1* SSKO skin feature increased neutrophil abundance and decreased T cell presence

Next, we performed flow cytometry to compare the immune cell compositions between IMQ-treated control and *Ovol1* SSKO mice. At 24 hours after the second IMQ treatment, we detected a ~3.7-fold increase in neutrophils (CD45<sup>+</sup>/Ly6G<sup>+</sup>/CD11b<sup>+</sup>) in *Ovol1* SSKO skin compared with that in the control littermate skin, whereas similar numbers of total immune (CD45<sup>+</sup>) cells and macrophages (CD45<sup>+</sup>/F4/80<sup>+</sup>/CD11b<sup>+</sup>/Ly6G<sup>-</sup>) were observed (Figure 2a and b and Supplementary Figure S2a). These data show that loss of epidermal expression of *Ovol1* results in an increased early influx of neutrophils in IMQ-treated skin.

We also examined the impact of *Ovol1* deletion on components of the adaptive immune response, which generally develops around 5–14 days after IMQ treatment (Miao et al.,

2010). Specifically, we employed two consecutive IMQ applications to minimize indirect consequences from dramatic epidermal thickening and barrier disruption (Supplementary Figure S1a and b) and performed flow cytometry 6 days later. Compared with those in the control counterparts, the average numbers of both CD45<sup>+</sup> (immune) and CD45<sup>-</sup> cells were increased in Ovol1 SSKO skin, but the differences were not statistically significant (Figure 2c and Supplementary Figure S2b and c). Importantly, the percentage of CD3<sup>+</sup> lymphocytes (CD45<sup>+</sup>CD3/Thy1<sup>+</sup>) of total immune (CD45<sup>+</sup>) cells was significantly lower in Ovol1 SSKO skin than in control skin, whereas the percentage of nonlymphocytes was significantly elevated (Figure 2d and e). A significant reduction was observed for the relative abundance of both CD4<sup>+</sup> T cells and CD8<sup>-</sup>CD4<sup>-</sup> T cells (which likely includes xδT cells [Cai et al., 2011; Tigelaar et al., 1990]) subsets (Figure 2d and f), whereas the relative abundance of Tregs (CD4<sup>+</sup>Foxp3<sup>+</sup>) showed a trend of increase in the mutant mice (Figure 2g and Supplementary Figure S2c and d). All these differences were normalized 1–3 months after IMQ treatment (Supplementary Figure S2e-h). Collectively, these data show that loss of epidermal Ovol1 biases the skin's response to IMQ toward elevated neutrophil accumulation but reduced T cell abundance.

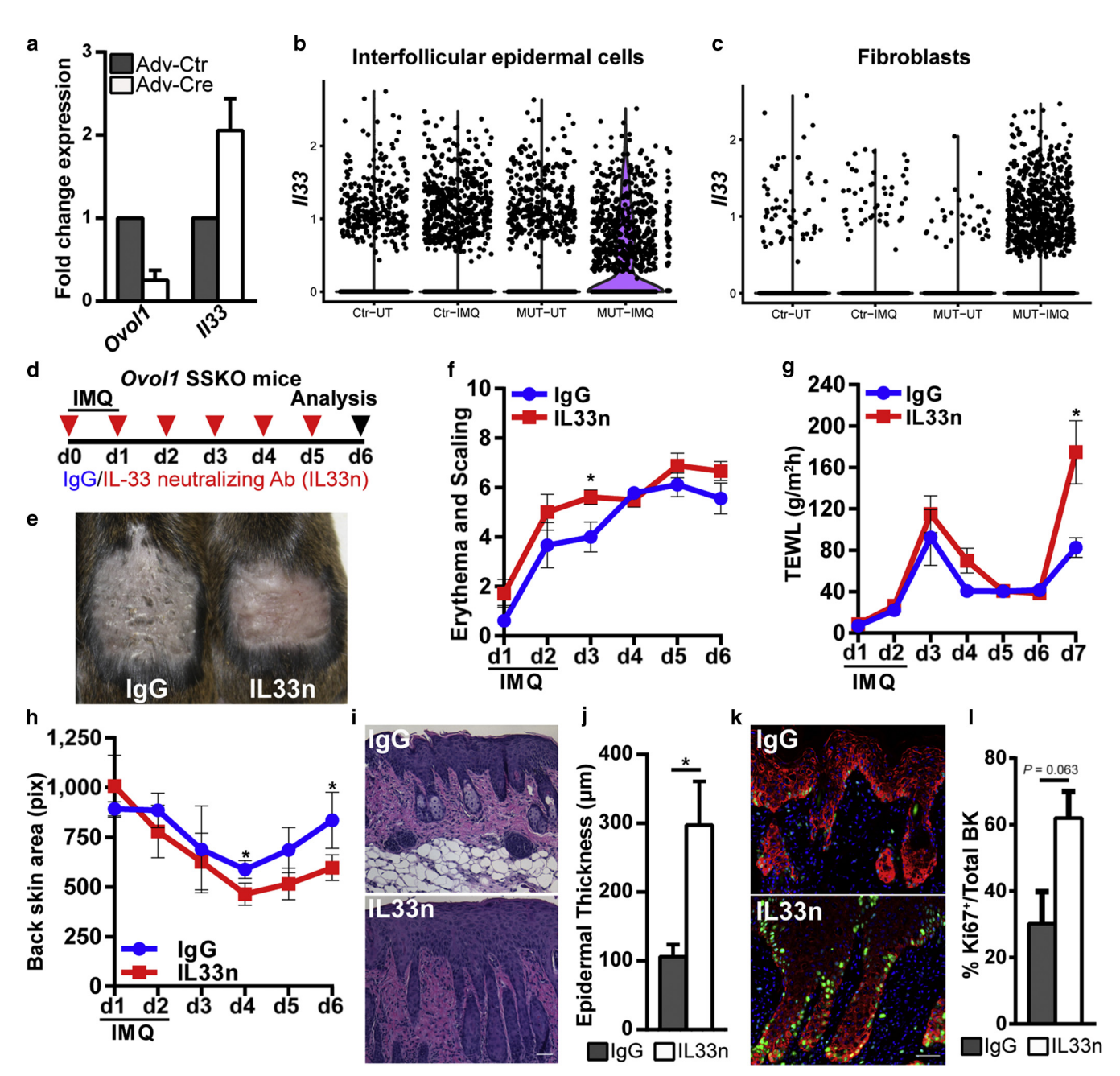


Figure 3. Expression and function of *Il33* in *Ovol1*-deficient skin. (a) RT-qPCR analysis on primary mouse keratinocytes derived from  $Ovol1^{iff}$  mice and infected with Adv-Ctr or Adv-Cre. Results from a single experiment are shown but are representative of three independent experiments. (b, c) Violin plots showing the expression of *Il33* in (b) interfollicular epidermal cells or (c) fibroblasts from scRNA-seq datasets (Sun et al., 2021). (d) The design of experiments for IL-33—neutralizing Ab (IL33n) or IgG control on *Ovol1* SSKO mice in e-I. (e) The external appearance of the skin on d6. (f-h) Time courses showing (f) phenotype progression, (g) TEWL measurements, and (h) treated back skin area (using the images in Supplementary Figure S3e). (i) Skin histology and (j) quantification of epidermal thickness on d6. Bar = 50  $\mu$ m. (k) Immunofluorescence and (l) quantification of proliferative basal (Ki-67+K14+) cells on d6. n = 3 pairs of IgG- and IL33n-treated *Ovol1* SSKO mice. \* P < 0.05. Error bars represent (a, g, j, l) mean  $\pm$  SD and (f, h) SEM. Ab, antibody; Adv-Cre, Cre-expressing adenovirus; Adv-Ctr, control adenovirus; BK, basal keratinocytes; d, day; IMQ, imiquimod; K, keratin; MUT, mutant; pix, pixel; scRNA-seq, single-cell RNA sequencing; SSKO, skin epithelia—specific knockout; TEWL, transepidermal water loss; UT, untreated; Ctr, control.

# Ovol1 loss results in elevated Il33 expression in inflamed skin, and inhibition of IL-33 signaling aggravates the IMQ-induced skin phenotypes of Ovol1 SSKO mice

IL-33, a cytokine of the IL-1 family that is expressed in barrier tissues, has been identified as a risk factor and modulator of psoriatic inflammation (Balato et al., 2012; Duan et al., 2019; Griesenauer and Paczesny, 2017; Pichery et al., 2012). To seek the potential targets of Ovol1 in the epidermis of

inflamed skin, we first considered *II33* as a candidate because recent reports show that *OVOL1* depletion in normal human epidermal KCs induces *IL33* expression (Tsuji et al., 2020). We found that both knockdown of *OVOL1* in normal human epidermal KCs and adenovirus Cre-mediated acute knockout of *Ovol1* in primary mouse KCs derived from *Ovol1*<sup>ff</sup> mice resulted in elevated *IL33/II33* expression (Figure 3a and Supplementary Figure S3a). Thus, similar to

OVOL1 in humans, Ovol1 is capable of suppressing *Il33* expression in mouse epidermal cells.

Next, we asked whether the loss of Ovol1 alters II33 expression in vivo. Interrogation of our previously published RNA-sequencing data on control and Ovol1<sup>-/-</sup> epidermis 6 hours after IMQ treatment (Sun et al., 2021) revealed elevated 1133 expression in the epidermis from Ovol1<sup>-/-</sup> mice ( $\times 3.2$ ,  $P < 10^{-5}$ ). Having said this, RT-qPCR showed only a statistically nonsignificant increase for *Il33* expression in IMQ-treated Ovol1<sup>-/-</sup> epidermis, whereas the increased expression of Il1a was significant (Supplementary Figure S3b). We also analyzed our published single-cell RNA-sequencing data on control and Ovol1<sup>-/-</sup> mice 24 hours after IMQ treatment (Sun et al., 2021). In the interfollicular epidermis, 1133 was found to be predominantly expressed by basal KCs, and the number of 1/33-expressing basal cells increased in the mutant after IMQ treatment compared with that in the control (Figure 3b and Supplementary Figure S3c-e). Moreover, control fibroblasts rarely showed detectable 1133 expression, but fibroblasts from Ovol1<sup>-/-</sup> mice became II33-positive after IMQ treatment (Figure 3c). Finally, RT-qPCR on RNAs isolated from the whole skin of control and Ovol1 SSKO mice revealed potential increases 6 hours and 2-3 days as well as a statistically significant increase 6 days after IMQ treatment for II33 expression (Kakkar and Lee, 2008) (Supplementary Figure S3f). Taken together, these results suggest that epidermal loss of Ovol1 results in mildly elevated expression of 1/33 in the epidermis but remarkably increased expression in the dermis of inflamed skin.

To investigate the effect of excessive 1/33 expression in the psoriasis-like microenvironment of IMQ-treated Ovol1-deficient mice, we intraperitoneally injected Ovol1 SSKO mice with either IgG control or an IL-33-neutralizing antibody (Byrne et al., 2011; Liu et al., 2016; Ohno et al., 2011; Peng et al., 2018; Schmitz et al., 2005) before and every day succeeding two IMQ applications (Figure 3d). Interestingly, neutralization of IL-33 signaling led to more severe skin defects characterized by exacerbated erythema and scaling, enhanced epidermal barrier disruption, and apparent contraction of the IMQ-treated skin area (Figure 3e-h and Supplementary Figure S3g-i). Consistent with enhanced epidermal hyperplasia at a histological level (Figure 3i and j), Ki-67 immunostaining trended toward elevated proliferative activity in the epidermal basal layer, including cells lining the finger-like projections (Figure 3k and I). However, the expression of keratin 1 and loricrin appeared unchanged (Supplementary Figure S3j and k), suggesting that the process of epidermal terminal differentiation is not affected by IL-33 neutralization. Despite previous reports of IL-33's effects on immune cell populations such as Tregs and neutrophils in other inflammatory models (Enoksson et al., 2013; Griesenauer and Paczesny, 2017; Lan et al., 2016; Matta et al., 2014), we did not detect any statistically significant change in nonlymphocytes and various T cell populations (including Tregs) after IL-33 neutralization in our model (Supplementary Figure S31-p). Collectively, these data suggest that the upregulated expression of Il33 in Ovol1 SSKO skin functions to suppress rather than enhance the IMQinduced skin phenotypes and epidermal hyperplasia.

# Identification of an *Ovol1-Cxcl1*-neutrophil regulatory axis that enhances IMQ-induced skin inflammation in *Ovol1* SSKO mice

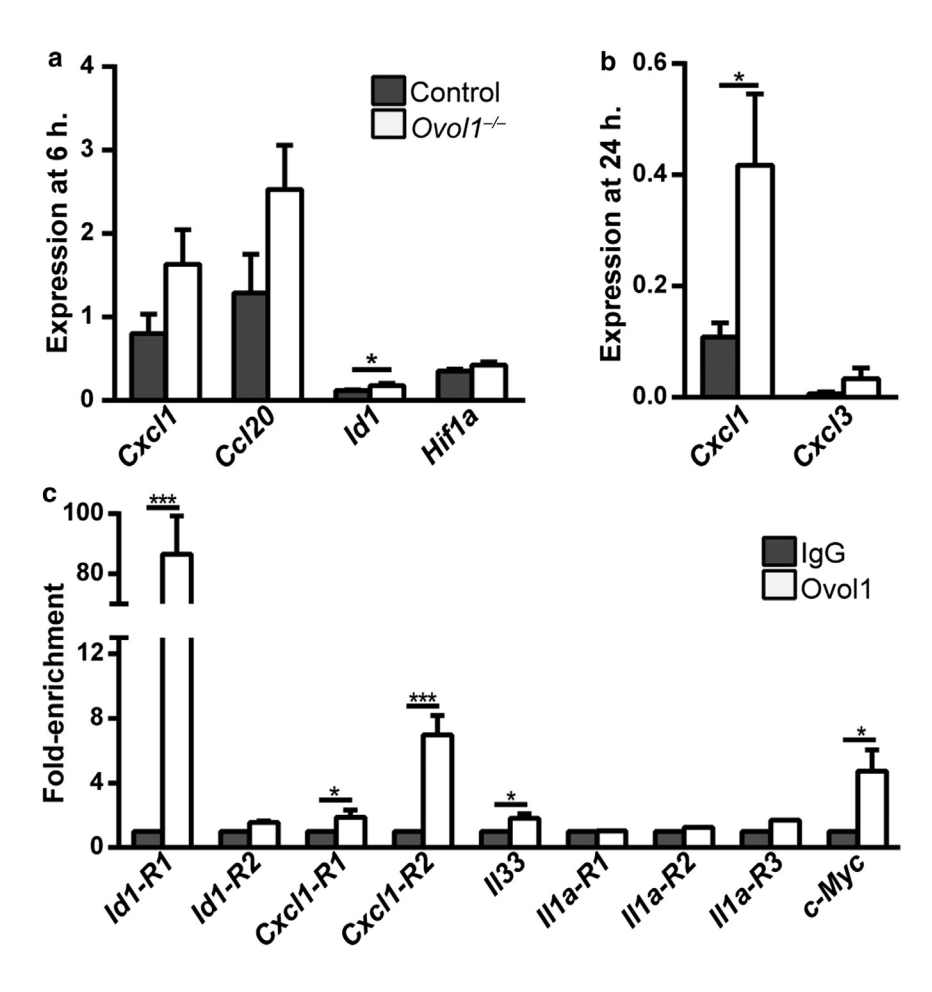
To seek additional candidate targets that mediate the enhanced inflammation in Ovol1-deficient skin, we returned to the RNA-sequencing data on IMQ-treated  $Ovol1^{-/-}$  and control epidermis (Sun et al., 2021), this time focusing on the chemokines known to be involved in neutrophil recruitment. We found Cxcl1 (×2.1), Cxcl2 (×3.0), and Cxcl3 (×3.1) to be significantly increased in IMQ-treated  $Ovol1^{-/-}$  epidermis ( $P<10^{-6}$ ). RT-qPCR analysis using independent samples confirmed the increased expression of Cxcl1 in  $Cvol1^{-/-}$  epidermis both 6 and 24 hours after IMQ treatment, with the upregulation being more dramatic and statistically significant at 24 hours (Figure 4a and b). A possible increase in Cxcl3 expression was also observed (Figure 4b).

Ovol1 encodes a transcriptional repressor (Nair et al., 2007, 2006). Thus, genes that were upregulated in its absence might be direct Ovol1 targets. Indeed, the Cxcl1 gene but not Cxcl2/3 contains OVOL1-binding consensus motifs (CCGTTA) (Nair et al., 2007) at two different regions (R1, -3505 to -3411; R2, +1262 - +1355). To validate Ovol 1 binding, we performed chromatin immunoprecipitation coupled with real-time qPCR on epidermal cells isolated from wild-type mice 2-6 hours after IMQ treatment. Chromatin immunoprecipitation coupled with real-time qPCR revealed strong Ovol1 binding to the promoter of a known Ovol1 target, *Id1* (Renaud et al., 2015), at -1073 to -997 (R1) but not at another site (R2, +1269 - +1368) (Figure 4c). Binding to another known Ovol1 target, c-Myc (Nair et al., 2006), was also detected. Importantly, chromatin immunoprecipitation coupled with real-time qPCR revealed Ovol1 binding to the Cxcl1 gene at both predicted sites (Figure 4c). Weak but statistically significant Ovol1 enrichment was also detected upstream of the 1133 promoter at a region (-1986 to -1903) that contains an Ovol1-binding consensus motif. In contrast, no enrichment was seen for Il1a at three different regions (R1-R3). These results suggest that Cxcl1 is a strong candidate as a direct Ovol1 target in skin epidermis, whereas 1/33 and 1/1a are likely weakly or indirectly regulated by

The identification of *Cxcl1* as a potential Ovol1 target led us to look more closely at neutrophil dynamics in inflamed skin with *Ovol1* ablation. At 6 hours after the first IMQ application, sizable neutrophil clusters (Ly6G positive) were already formed in *Ovol1* SSKO skin near the epidermis but were lacking in control littermates (Figure 5a). In *Ovol1*—mice, neutrophils were detected in the dermis 6 hours after IMQ treatment, whereas visible large neutrophil aggregates were observed 12–72 hours after IMQ at locations near, across, and atop the epidermis (Figure 5b). At all time points examined, only scattered neutrophils were detected around the epidermis of control counterparts (Figure 5b). These data provide evidence that loss of *Ovol1* in the epidermis results in increased neutrophil accumulation, trafficking, and abscess formation near the epidermis of IMQ-treated skin.

To assess the functional contribution of neutrophils to IMQ-induced skin pathology of *Ovol1*-deficient mice, we depleted neutrophils using a neutralizing antibody against Ly6G (Daley et al., 2008) (Figure 5c). Both immunostaining

Figure 4. Molecular analysis of OVOL1 targets in the epidermis. (a, b) RT-qPCR analysis at (a) 6 and (b) 24 h after IMQ treatment. n = 5 for Ovol1<sup>-/-</sup> and 4 for control littermates in a; note that two pairs of these mice were also used for RNA-seq analysis. n = 5 pairs in **b**. (c) ChIP-qPCR for the indicated genes in epidermal cells isolated from 2-6 h post-IMQ-treated adult skin. IgG control values were normalized to 1 for all. Results are summarized from one to four independent experiments. \*\*\* P < 0.005; \* P < 0.05. P-values were calculated using a two-tailed Student's paired t-test. Error bars represent mean ± SEM. ChIP-qPCR, chromatin immunoprecipitation coupled with real-time qPCR; h, hour; IMQ, imiquimod; RNA-seq, RNA sequencing.



and histological analysis revealed a reduced presence of neutrophils in IMQ-treated *Ovol1*<sup>-/-</sup> skin after Ly6G antibody injection relative to that after IgG injection (Figure 5d and Supplementary Figure S4a). Epidermal thickness and the number of Ki-67—positive basal cells were not significantly different between IgG- and Ly6G antibody—injected skin at the endpoint of these experiments (day 3 after IMQ treatment) (Supplementary Figure S4b and c). However, external symptoms such as erythema and scaling/plaque formation in *Ovol1*<sup>-/-</sup> mice were significantly improved by Ly6G antibody injection (Figure 5e and f and Supplementary Figure S4d). These effects show that the accumulated neutrophils in *Ovol1*-deficient skin functionally contribute to IMQ-induced erythema and scaling/plaque formation.

#### **DISCUSSION**

Our work unravels previously unknown mechanisms by which an epidermal KC-intrinsic transcription factor modulates innate and adaptive immune responses in the skin in tandem with barrier maintenance. When the skin is chemically challenged or mechanically disrupted, Ovol1 helps to maintain a functional barrier to protect from such perturbations. It likely does so by regulating the proliferation and differentiation of epidermal cells by repressing the expression of genes such as *Ovol1*, *c-Myc* (Nair et al., 2007), *Ovol2* (Teng et al., 2007), *Flg* (Tsuji et al., 2017), and *Id1* (this work). Importantly, our work identifies a role for epidermally

expressed Ovol1 to directly and indirectly regulate the expression of cytokines and chemokines such as *II1a, II33,* and *CxcI1,* thereby modulating the ensuing immune response.

Interestingly, the epidermal hyperplasia in IMQ-treated Ovol1 SSKO mice appeared more severe than that in IMQtreated Ovol1-/- mice (Sun et al., 2021). Moreover, neutrophil accumulation kinetics appears more rapid in Ovol1 SSKO skin than in  $Ovol1^{-/-}$  skin. It is possible that this is due to differential IMQ responses of B6 versus of CD1 backgrounds (Swindell et al., 2017, 2011). Alternatively, nonepidermal cells in Ovol1<sup>-/-</sup> mice might play a modulatory role in the IMQ responses. In human psoriatic skin, neutrophils infiltrate into the dermis from blood vessels at the early inflammatory phase and migrate into the epidermis at the chronic phase of psoriasis (Albanesi et al., 2010). Neutrophil dynamics in inflamed tissues beyond neutrophil-vasculature interactions is an emerging area of research, and swarm-like migration patterns, termed neutrophil swarming, have been described in various tissue and disease contexts (Kienle and Lämmermann, 2016). The slower neutrophil kinetics in the Ovol1<sup>-/-</sup> model enabled our discovery that initial dermal infiltration of neutrophils does not depend on Ovol1, whereas Ovol1 loss primarily affects the accumulation of neutrophils near or at the epidermis and the migration through the epidermis to form abscesses with KCs. Our data suggest that Ovol1 expression in the epidermis constitutes a protective mechanism that prevents epidermal-proximal

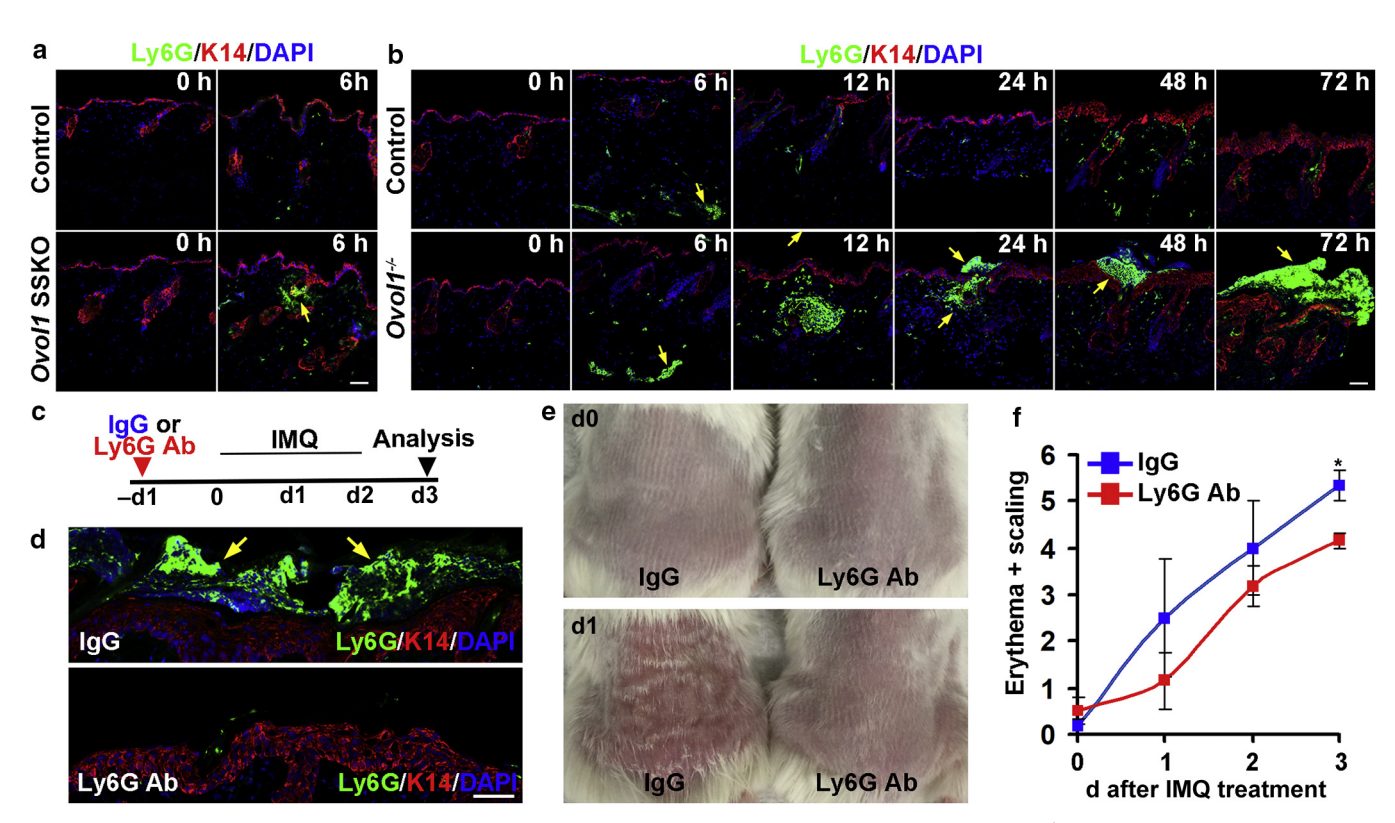


Figure 5. *Ovol1* loss alters neutrophil dynamics, and neutrophil depletion rescues psoriasis-like phenotypes in  $Ovol1^{-/-}$  skin. (a, b) Shown are representative images of immunostaining in (a) Ovol1 SSKO and (b)  $Ovol1^{-/-}$  mice. (a, b, d) Arrows point to neutrophils. (c) Design of neutrophil depletion experiments in d–f. IgG was used as a control. (d) Immunostaining on d3. (a, b) Bar = 50  $\mu$ m and (d) Bar = 100  $\mu$ m. (e) External appearance and (f) phenotypic score (n = 3) at the respective times. \*P < 0.05. Error bars represent mean  $\pm$  SEM. Ab, antibody; d, day; h, hour; IMQ, imiquimod; K, keratin; SSKO, skin epithelia–specific knockout.

neutrophil accumulation and abscess formation in inflamed skin. Combined with our previous study (Sun et al., 2021), we propose that Ovol1 does so by direct transcriptional repression of *Cxcl1* expression in KCs and by maintaining a robust barrier, which in turn suppresses KC expression of *Il1a* (Rider et al., 2011; Sawant et al., 2015; Sun et al., 2021). Although a possibility for this type of regulation was suggested (Hwang et al., 2011), to our knowledge, this study presents a previously unreported example of an epidermally expressed transcription factor modulating neutrophil behaviors in skin inflammation through direct target gene regulation.

Previous studies predominantly suggest a pro-inflammatory role of IL-33 in psoriasis (Balato et al., 2014; Duan et al., 2019; Miller et al., 2010; Sehat et al., 2018; Theoharides et al., 2010). However, it was recently reported that the introduction of recombinant IL-33 suppresses psoriatic inflammation and epidermal hyperplasia (Chen et al., 2020). Our results are consistent with this notion and suggest a protective role for IL-33 in the Ovol1-deficient mouse model against IMQ responses. It is possible that this protective function only manifests when the amount of IL-33 is excessive. IL-33 is an alarmin that can function both as a traditional cytokine (through receptor signaling) and as a nuclear transcriptional regulator (Haraldsen et al., 2009). Our antibody neutralization data implicate the signaling function of IL-33 in suppressing IMQ responses when Ovol1 and barrier are deficient. In other tissues, IL-33 can recruit a particularly suppressive form of Tregs through the ST2 receptor (Halvorsen et al., 2019; Pastille et al., 2019; Siede et al., 2016). However, despite a trending increase of Tregs in Ovol1 SSKO mice, after neutralizing IL-33, the total number of Tregs (including the ST2<sup>+</sup> subset) did not drastically vary. In this context, the IL-33/ST2 signaling axis may alter cytokine production by Tregs or other immune cells rather than recruiting or inducing Treg proliferation (Hemmers et al., 2021). In T helper type 2 allergic response, IL-33 can induce immune cells to release secreted proteins that induce the proliferation of KCs (Ryu et al., 2015), potentially explaining the epidermal hyperplasia that we observed. Alternatively, KCs in Ovol1-deficient mice may respond directly to excessive IL-33 signals and hyperproliferate because ST2L and pathways such as extracellular signal-regulated kinase and c-Jun N-terminal kinase are activated by IL-33 (Du et al., 2016). Although future work outside the scope of this study is needed to characterize the downstream cellular and molecular mediators of IL-33 function, our findings identify OVOL1 as an upstream regulator that directly suppresses 1133 expression in mice.

Collectively, this study adds Ovol1 to a growing list of skin barrier–protective transcription factors (Cangkrama et al., 2013; Gordon et al., 2014; Hwang et al., 2011; Koegel et al., 2009; Li et al., 2017; Lin et al., 2013; Segre et al., 1999) but highlights its unique role in the adult epidermis to promote barrier robustness under external challenges in coordination with fine-tuning epidermal–immune cell cross-talk. In an *Ovol1*-deficient skin microenvironment,

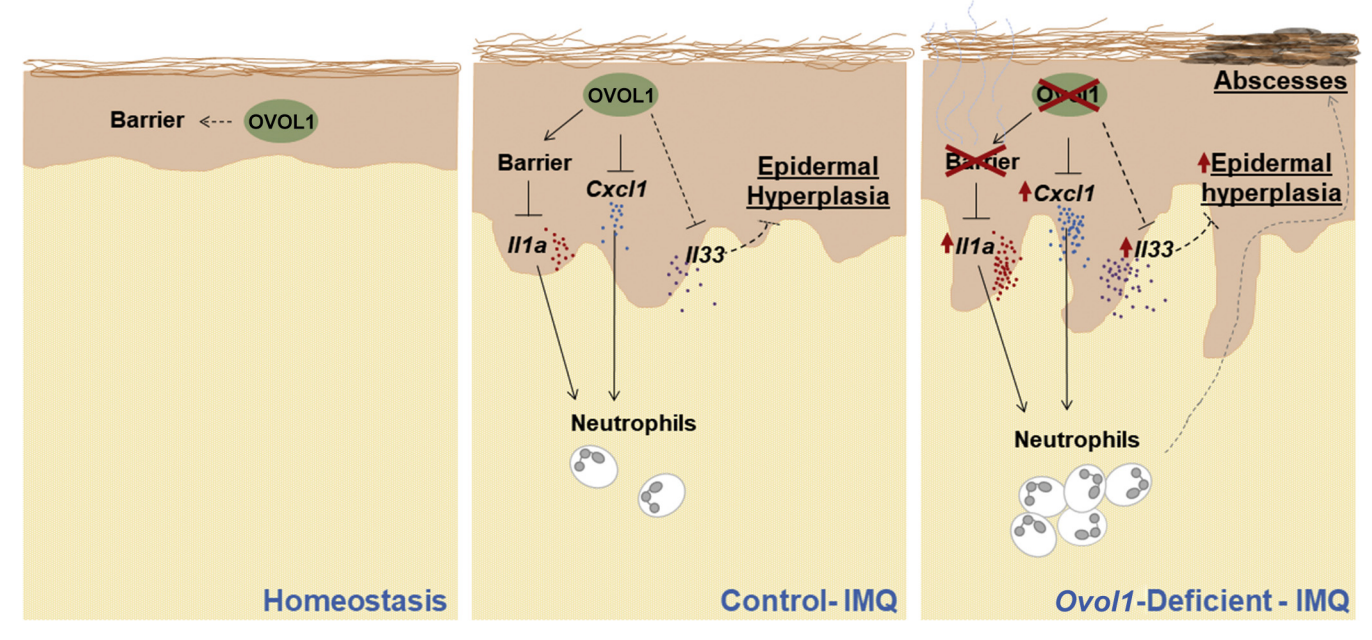


Figure 6. Working model of OVOL1 function in IMQ-induced skin inflammation. In normal skin treated with IMQ, epidermally expressed Ovol1 not only promotes barrier maintenance, thereby suppressing alarmin (IL-1α) production, but also directly represses the gene expression of *Cxcl1* chemokine and possibly *Il33* cytokine to modulate the inflammatory and hyperproliferative responses. In *Ovol1*-deficient skin treated with IMQ, the barrier is disrupted and, *Il1a* and *Cxcl1* are upregulated, resulting in excessive and persistent neutrophil accumulation and exacerbated inflammation. In contrast, *Il33* is upregulated likely as a protective mechanism to suppress excessive epidermal hyperplasia. IMQ, imiquimod.

both anti-inflammatory (*II33*) and proinflammatory (*Cxcl1*, *II1a*, neutrophils) components are upregulated and functionally contribute to skin pathology (Figure 6). These data underscore *Ovol1* function as part of a self-limiting, counterbalancing KC-intrinsic mechanism that maintains inflammation competence but at the same time keeps inflammation in check to restore tissue homeostasis. Dissecting the intricate and complex control of psoriasis-like inflammation by epidermal KCs sheds light on our understanding of psoriasis pathogenesis in human patients.

# MATERIALS AND METHODS

#### Mice

B6N-Ovol1<sup>tm1a(KOMP)Wtsi/J</sup> mice, where a cassette composed of an FRT site—a LacZ sequence—and loxP sites are inserted into the Ovol1 locus, were purchased from Knockout Mouse Project Repository of the University of California, Davis (Davis, CA). These mice were crossed with B6.Cg-Tg(ACTFLPe)9205Dym/J (Rodriguez et al., 2000) mice to generate a floxed (i.e., f) Ovol1 allele. Ovol1<sup>+/-</sup>; K14-Cre males were crossed with Ovol1<sup>iff</sup> females to generate Ovol1 SSKO (Ovol1<sup>i/-</sup>; K14-Cre) mice, which were then analyzed along with their sex- and weight-matched control littermates. Genotyping primers are provided in Supplementary Table S1. All animal studies have been approved and abide by the regulatory guidelines of the Institutional Animal Care and Use Committee of the University of California, Irvine (Irvine, CA).

## IMQ-induced psoriasis model

Mice aged 7—8 weeks received a daily topical dose of 62.5 mg 5% IMQ cream (Perrigo, Dublin, Ireland) on shaved backs for 1–5 consecutive days or as indicated. Additional details are described in the Supplementary Materials and Methods.

# Tape stripping and TEWL measurement

Tape stripping was performed as described in a study by Bruhs et al. (2018). In brief, hairs were removed from the mouse back by shaving. Three days later, shaved back skin was stripped with adhesive cellophane tape 20 times. For each stripping, a fresh piece of tape was lightly pressed onto the back and gently pulled off.

TEWL was measured on shaved mouse back skin using the Delfin VapoMeter (SWL4400, Delfin, Kuopio, Finland) under basal conditions (untapped or untreated), after tape stripping, or after two-time IMQ applications. TEWL values are output as g/m²h.

## Flow cytometry

T cells were isolated as described in the study by Ali et al. (2017). Whole skin was digested in 2% collagenase, 0.5 mg/ml hyaluronidase, and 0.1 mg/ml DNase in RPMI with 1% 4-(2-hydroxyethyl)-1piperazineethanesulfonic acid, 1% penicillin-streptomycin, and 10% fetal calf serum at 37 °C for 45 minutes. Cells were filtered through 70- and 40-µm filters, rinsed in 5% fetal bovine serum/ ×1PBS, and stained for 10 minutes with Zombie NIR (423105; BioLegend, San Diego, CA). Cells were stained with cell surface markers and anti-mouse CD16/32 (101320; BioLegend) in FACS buffer (5% fetal bovine serum/×1PBS) on ice for 30 minutes. Cells were fixed with the Transcription Factor Staining Buffer Set (00-5523-00; eBioscience, Waltham, MA), stained for eFluor450 anti-Foxp3 (48-5773-82; eBioscience) for 1 hour at room temperature, and then analyzed on a FACS Aria Fusion. Surface markers include APC anti-CD45 (103112; BioLegend), PerCP/Cy5.5 anti-CD3 (100218; BioLegend), and anti-CD90.2 (140322; BioLegend), FITC anti-CD8a (100705; BioLegend), BV605 anti-CD4 (100548; Bio-Legend), and phycoerythrin anti-ST2 (145303; BioLegend). Additional details are described in the Supplementary Materials and Methods.

# Chromatin immunoprecipitation coupled with real-time qPCR

The back skin of B6 mice was shaved and treated with IMQ for 2–6 hours. To separate epidermis from dermis, back skin was collected and digested with 2.5 U/ml dispase (07913; Stem Cell Technologies, Vancouver, Canada) for 1 hour at 37 °C, scraped, minced, resuspended in 5% fetal bovine serum/×1PBS, and filtered through 70-µm and 40-µm filters. Epidermal cells in single-cell suspension were then cross-linked in 1% formaldehyde, followed by chromatin immunoprecipitation assay using rabbit anti-OVOL1 antibody (Dai et al., 1998) and SimpleChIP Enzymatic Chromatin IP Kit (Agarose Beads) (9002; Cell Signaling Technology, Danvers, MA) according to manufacturer's instructions. DNA was then purified, and qPCR was performed using SYBRgreen reagent (Qiagen, Hilden, Germany) and gene-specific primers (Supplementary Table S1).

# In vivo administration of IL-33-neutralizing and anti-Ly6G antibodies

For IL-33 neutralization experiments, same-sex/same-weight Ovol1 SSKO littermates were intraperitoneally injected with 15 µg of goat anti-mouse IL-33 Affinity Purified Polyclonal antibody (AF3626; R&D Systems, Minneapolis, MN) or goat IgG (AB0108-C; R&D Systems) 30 minutes before the two IMQ applications and at the same time of the day for a total of six applications. For neutrophil depletion studies, same-sex/same-weight Ovol1<sup>-/-</sup> littermates were intraperitoneally injected with 500 µg rat anti-mouse Ly-6G antibody (clone 1A8, eBioscience) or rat IgG2a (clone eBR2a, eBioscience) once 24 hours before IMQ application. In separate control experiments, same-sex/same-weight wild-type littermates were also treated and analyzed. Skin was harvested either 6 days after the first IMQ treatment (IL-33 neutralizing) or 24 hours after the third IMQ treatment (for Ly6G) and was fixed in 4% paraformaldehyde for H&E staining, embedded in optimum cutting temperature, and frozen for immunostaining, or single cells were isolated for flow cytometry analysis.

## Statistics and reproducibility

Nearly all experiments were performed on at least three biological replicates or repeated at least twice. The sample size and number of independent experiments are indicated in the relevant figure legends. Disease pathology scoring was performed blindly. No data were excluded. For analysis of the differences between groups, Student's unpaired two-tailed *t*-test was performed in Excel unless otherwise indicated. *P*-values of 0.05 or less were considered statistically significant and are indicated in the figures/legends. Those where *P*-values are not indicated are not statistically significant.

Additional information is provided in Supplementary Materials and Methods.

#### Data availability statement

No datasets were generated during this study. The analysis uses previously published datasets (Sun et al., 2021).

#### **ORCID**

Morgan Dragan: http://orcid.org/0000-0002-6401-6816
Peng Sun: http://orcid.org/0000-0001-9858-6537
Zeyu Chen: http://orcid.org/0000-0001-6393-1986
Xianghui Ma: http://orcid.org/0000-0002-6171-0722
Remy Vu: http://orcid.org/0000-0002-1283-0728
Yuling Shi: http://orcid.org/0000-0002-1273-7881
S. Armando Villalta: http://orcid.org/0000-0002-5212-2259
Xing Dai: http://orcid.org/0000-0001-8134-1365

#### **CONFLICT OF INTEREST**

The authors state no conflict of interest.

#### **ACKNOWLEDGMENTS**

We thank Bogi Andersen for use of the Vapometer and the Institute for Immunology FACS Core Facility at the University of California, Irvine for expert service. This work was supported by National Institutes of Health Grants R01-AR068074 and R01-GM123731 (XD). MD is partially supported by the National Institutes of Health T32 Immunology Research Training Grant (AI 060573). ZC was supported by the China Scholarship Council (Grant No. 201906260233). RV was supported by the National Science Foundation GRFP (DGE-1839285).

#### **AUTHOR CONTRIBUTIONS**

Conceptualization: XD; Data Curation: MD, PS, ZC, XM; Formal Analysis: MD, PS, ZC, XM, RV; Funding Acquisition: XD; Investigation: MD, PS, ZC, XM; Validation: MD, PS, ZC, XM; Project Administration: XD; Supervision: XD, YS, SAV; Visualization: MD, PS, ZC, XM; Writing - Original Draft Preparation: XD, MD; Writing - Review and Editing: XD, MD, PS, ZC, XM, YS, SAV

#### **SUPPLEMENTARY MATERIALS**

Supplementary material is linked to the online version of the paper at www. jidonline.org, and at https://doi.org/10.1016/j.jid.2021.08.397.

#### **REFERENCES**

- Albanesi C, Scarponi C, Bosisio D, Sozzani S, Girolomoni G. Immune functions and recruitment of plasmacytoid dendritic cells in psoriasis. Autoimmunity 2010;43:215–9.
- Alexander H, Brown S, Danby S, Flohr C. Research techniques made simple: transepidermal water loss measurement as a research tool. J Invest Dermatol 2018;138:2295–300.e1.
- Ali N, Zirak B, Rodriguez RS, Pauli ML, Truong HA, Lai K, et al. Regulatory T cells in skin facilitate epithelial stem cell differentiation. Cell 2017;169: 1119–29.e11.
- Balato A, Di Caprio R, Canta L, Mattii M, Lembo S, Raimondo A, et al. IL-33 is regulated by TNF- $\alpha$  in normal and psoriatic skin. Arch Dermatol Res 2014;306:299–304.
- Balato A, Lembo S, Mattii M, Schiattarella M, Marino R, De Paulis A, et al. IL-33 is secreted by psoriatic keratinocytes and induces pro-inflammatory cytokines via keratinocyte and mast cell activation [published correction appears in Exp Dermatol 2012;21:892–4.
- Barland CO, Zettersten E, Brown BS, Ye J, Elias PM, Ghadially R. Imiquimodinduced interleukin-1 alpha stimulation improves barrier homeostasis in aged murine epidermis. J Invest Dermatol 2004;122:330—6.
- Bruhs A, Proksch E, Schwarz T, Schwarz A. Disruption of the epidermal barrier induces regulatory T cells via IL-33 in mice. J Invest Dermatol 2018;138:570–9.
- Byrne SN, Beaugie C, O'Sullivan C, Leighton S, Halliday GM. The immune-modulating cytokine and endogenous alarmin interleukin-33 is upregulated in skin exposed to inflammatory UVB radiation. Am J Pathol 2011;179:211–22.
- Cai Y, Shen X, Ding C, Qi C, Li K, Li X, et al. Pivotal role of dermal IL-17-producing  $\gamma\delta$  T cells in skin inflammation [published correction appears in Immunity 2011;35:549]. Immunity 2011;35:596–610.
- Cangkrama M, Ting SB, Darido C. Stem cells behind the barrier. Int J Mol Sci 2013;14:13670–86.
- Chen Z, Hu Y, Gong Y, Zhang X, Cui L, Chen R, et al. Interleukin-33 alleviates psoriatic inflammation by suppressing the T helper type 17 immune response. Immunology 2020;160:382–92.
- Chiang CC, Cheng WJ, Korinek M, Lin CY, Hwang TL. Neutrophils in psoriasis. Front Immunol 2019;10:2376.
- Dai X, Schonbaum C, Degenstein L, Bai W, Mahowald A, Fuchs E. The ovo gene required for cuticle formation and oogenesis in flies is involved in hair formation and spermatogenesis in mice. Genes Dev 1998;12:3452–63.
- Daley JM, Thomay AA, Connolly MD, Reichner JS, Albina JE. Use of Ly6G-specific monoclonal antibody to deplete neutrophils in mice. J Leukoc Biol 2008;83:64–70.
- Du HY, Fu HY, Li DN, Qiao Y, Wang QW, Liu W. The expression and regulation of interleukin-33 in human epidermal keratinocytes: a new mediator of atopic dermatitis and its possible signaling pathway. J Interferon Cytokine Res 2016;36:552–62.

- Duan Y, Dong Y, Hu H, Wang Q, Guo S, Fu D, et al. IL-33 contributes to disease severity in psoriasis-like models of mouse. Cytokine 2019;119: 159–67.
- Enoksson M, Möller-Westerberg C, Wicher G, Fallon PG, Forsberg-Nilsson K, Lunderius-Andersson C, et al. Intraperitoneal influx of neutrophils in response to IL-33 is mast cell-dependent. Blood 2013;121:530–6.
- Furue K, Ito T, Tsuji G, Ulzii D, Vu YH, Kido-Nakahara M, et al. The IL-13-OVOL1-FLG axis in atopic dermatitis. Immunology 2019;158: 281-6.
- Gonzales KAU, Fuchs E. Skin and its regenerative powers: an alliance between stem cells and their niche. Dev Cell 2017;43:387–401.
- Gordon WM, Zeller MD, Klein RH, Swindell WR, Ho H, Espetia F, et al. A GRHL3-regulated repair pathway suppresses immune-mediated epidermal hyperplasia. J Clin Invest 2014;124:5205—18.
- Griesenauer B, Paczesny S. The ST2/IL-33 axis in immune cells during inflammatory diseases. Front Immunol 2017;8:475.
- Halvorsen EC, Franks SE, Wadsworth BJ, Harbourne BT, Cederberg RA, Steer CA, et al. IL-33 increases ST2 <sup>+</sup> Tregs and promotes metastatic tumour growth in the lungs in an amphiregulin-dependent manner. Oncoimmunology 2019;8:e1527497.
- Haraldsen G, Balogh J, Pollheimer J, Sponheim J, Küchler AM. Interleukin-33 cytokine of dual function or novel alarmin? Trends Immunol 2009;30: 227–33.
- Harden JL, Krueger JG, Bowcock AM. The immunogenetics of psoriasis: a comprehensive review. J Autoimmun 2015;64:66–73.
- Hemmers S, Schizas M, Rudensky AY. Treg cell-intrinsic requirements for ST2 signaling in health and neuroinflammation. J Exp Med 2021;218: e20201234.
- Hwang J, Kita R, Kwon HS, Choi EH, Lee SH, Udey MC, et al. Epidermal ablation of Dlx3 is linked to IL-17-associated skin inflammation. Proc Natl Acad Sci USA 2011;108:11566—71.
- Kakkar R, Lee RT. The IL-33/ST2 pathway: therapeutic target and novel biomarker. Nat Rev Drug Discov 2008;7:827–40.
- Kienle K, Lämmermann T. Neutrophil swarming: an essential process of the neutrophil tissue response. Immunol Rev 2016;273:76–93.
- Kobayashi T, Naik S, Nagao K. Choreographing immunity in the skin epithelial barrier. Immunity 2019;50:552–65.
- Koegel H, von Tobel L, Schäfer M, Alberti S, Kremmer E, Mauch C, et al. Loss of serum response factor in keratinocytes results in hyperproliferative skin disease in mice. J Clin Invest 2009;119:899–910.
- Lan F, Yuan B, Liu T, Luo X, Huang P, Liu Y, et al. Interleukin-33 facilitates neutrophil recruitment and bacterial clearance in S. aureus-caused peritonitis. Mol Immunol 2016;72:74–80.
- Lee B, Villarreal-Ponce A, Fallahi M, Ovadia J, Sun P, Yu QC, et al. Transcriptional mechanisms link epithelial plasticity to adhesion and differentiation of epidermal progenitor cells. Dev Cell 2014;29:47–58.
- Li S, Teegarden A, Bauer EM, Choi J, Messaddeq N, Hendrix DA, et al. Transcription factor CTIP1/BCL11A regulates epidermal differentiation and lipid metabolism during skin development. Sci Rep 2017;7:13427.
- Lin C, Hindes A, Burns CJ, Koppel AC, Kiss A, Yin Y, et al. Serum response factor controls transcriptional network regulating epidermal function and hair follicle morphogenesis. J Invest Dermatol 2013;133:608–17.
- Liu B, Tai Y, Achanta S, Kaelberer MM, Caceres AI, Shao X, et al. IL-33/ST2 signaling excites sensory neurons and mediates itch response in a mouse model of poison ivy contact allergy. Proc Natl Acad Sci USA 2016;113: E7572–9.
- Matta BM, Lott JM, Mathews LR, Liu Q, Rosborough BR, Blazar BR, et al. IL-33 is an unconventional alarmin that stimulates IL-2 secretion by dendritic cells to selectively expand IL-33R/ST2+ regulatory T cells. J Immunol 2014:193:4010–20.
- Miao H, Hollenbaugh JA, Zand MS, Holden-Wiltse J, Mosmann TR, Perelson AS, et al. Quantifying the early immune response and adaptive immune response kinetics in mice infected with influenza A virus. J Virol 2010;84:6687–98.
- Miller AM, Asquith DL, Hueber AJ, Anderson LA, Holmes WM, McKenzie AN, et al. Interleukin-33 induces protective effects in adipose tissue inflammation during obesity in mice. Circ Res 2010;107: 650–8.

- Milora KA, Fu H, Dubaz O, Jensen LE. Unprocessed interleukin-36 $\alpha$  regulates psoriasis-like skin inflammation in cooperation with interleukin-1. J Invest Dermatol 2015;135:2992–3000.
- Murphy M, Kerr P, Grant-Kels JM. The histopathologic spectrum of psoriasis. Clin Dermatol 2007;25:524–8.
- Nair M, Bilanchone V, Ortt K, Sinha S, Dai X. Ovol1 represses its own transcription by competing with transcription activator c-Myb and by recruiting histone deacetylase activity. Nucleic Acids Res 2007;35:1687–97.
- Nair M, Teng A, Bilanchone V, Agrawal A, Li B, Dai X. Ovol1 regulates the growth arrest of embryonic epidermal progenitor cells and represses c-myc transcription. J Cell Biol 2006;173:253–64.
- Ohno T, Oboki K, Morita H, Kajiwara N, Arae K, Tanaka S, et al. Paracrine IL-33 stimulation enhances lipopolysaccharide-mediated macrophage activation. PLoS One 2011;6:e18404.
- Olaru F, Jensen LE. Staphylococcus aureus stimulates neutrophil targeting chemokine expression in keratinocytes through an autocrine IL-1alpha signaling loop. J Invest Dermatol 2010;130:1866—76.
- Pasparakis M, Haase I, Nestle FO. Mechanisms regulating skin immunity and inflammation. Nat Rev Immunol 2014;14:289–301.
- Pastille E, Wasmer MH, Adamczyk A, Vu VP, Mager LF, Phuong NNT, et al. The IL-33/ST2 pathway shapes the regulatory T cell phenotype to promote intestinal cancer. Mucosal Immunol 2019;12:990–1003.
- Peng G, Mu Z, Cui L, Liu P, Wang Y, Wu W, et al. Anti-IL-33 antibody has a therapeutic effect in an atopic dermatitis murine model induced by 2, 4-dinitrochlorobenzene. Inflammation 2018;41:154–63.
- Pichery M, Mirey E, Mercier P, Lefrancais E, Dujardin A, Ortega N, et al. Endogenous IL-33 is highly expressed in mouse epithelial barrier tissues, lymphoid organs, brain, embryos, and inflamed tissues: in situ analysis using a novel Il-33—LacZ gene trap reporter strain. J Immunol 2012;188: 3488—95.
- Pinkus H, Mehregan AH. The primary histologic lesion of seborrheic dermatitis and psoriasis. J Invest Dermatol 1966;46:109–16.
- Renaud SJ, Chakraborty D, Mason CW, Rumi MA, Vivian JL, Soares MJ. OVOlike 1 regulates progenitor cell fate in human trophoblast development. Proc Natl Acad Sci USA 2015;112:E6175—84.
- Rider P, Carmi Y, Guttman O, Braiman A, Cohen I, Voronov E, et al. IL-1 $\alpha$  and IL-1 $\beta$  recruit different myeloid cells and promote different stages of sterile inflammation. J Immunol 2011;187:4835–43.
- Ring J, Möhrenschlager M, Weidinger S. Molecular genetics of atopic eczema. Chem Immunol Allergy 2012;96:24–9.
- Rodríguez CI, Buchholz F, Galloway J, Sequerra R, Kasper J, Ayala R, et al. High-efficiency deleter mice show that FLPe is an alternative to Cre-loxP. Nat Genet 2000;25:139–40.
- Ryu Wl, Lee H, Kim JH, Bae HC, Ryu HJ, Son SW. IL-33 induces Egr-1-dependent TSLP expression via the MAPK pathways in human keratinocytes. Exp Dermatol 2015;24:857—63.
- Sawant KV, Xu R, Cox R, Hawkins H, Sbrana E, Kolli D, et al. Chemokine CXCL1-mediated neutrophil trafficking in the lung: role of CXCR2 activation. J Innate Immun 2015;7:647–58.
- Schmitz J, Owyang A, Oldham E, Song Y, Murphy E, McClanahan TK, et al. IL-33, an interleukin-1-like cytokine that signals via the IL-1 receptor-related protein ST2 and induces T helper type 2-associated cytokines. Immunity 2005;23:479—90.
- Schmuth M, Blunder S, Dubrac S, Gruber R, Moosbrugger-Martinz V. Epidermal barrier in hereditary ichthyoses, atopic dermatitis, and psoriasis. J Dtsch Dermatol Ges 2015;13:1119–23.
- Segre JA. Epidermal barrier formation and recovery in skin disorders. J Clin Invest 2006;116:1150–8.
- Segre JA, Bauer C, Fuchs E. Klf4 is a transcription factor required for establishing the barrier function of the skin. Nat Genet 1999;22:356–60.
- Sehat M, Talaei R, Dadgostar E, Nikoueinejad H, Akbari H. Evaluating serum levels of IL-33, IL-36, IL-37 and gene expression of IL-37 in patients with psoriasis vulgaris. Iran J Allergy Asthma Immunol 2018;17: 179–87.
- Siede J, Fröhlich A, Datsi A, Hegazy AN, Varga DV, Holecska V, et al. IL-33 receptor-expressing regulatory T cells are highly activated, Th2 biased and suppress CD4 T cell proliferation through IL-10 and TGF $\beta$  Release. PLoS One 2016;11:e0161507.

- Sumida H, Yanagida K, Kita Y, Abe J, Matsushima K, Nakamura M, et al. Interplay between CXCR2 and BLT1 facilitates neutrophil infiltration and resultant keratinocyte activation in a murine model of imiquimod-induced psoriasis. J Immunol 2014;192:4361–9.
- Sun P, Vu R, Dragan M, Haensel D, Gutierrez G, Nguyen Q, et al. OVOL1 regulates psoriasis-like skin inflammation and epidermal hyperplasia. J Invest Dermatol 2021;141:1542–52.
- Swindell WR, Johnston A, Carbajal S, Han G, Wohn C, Lu J, et al. Genomewide expression profiling of five mouse models identifies similarities and differences with human psoriasis. PLoS One 2011;6:e18266.
- Swindell WR, Michaels KA, Sutter AJ, Diaconu D, Fritz Y, Xing X, et al. Imiquimod has strain-dependent effects in mice and does not uniquely model human psoriasis. Genome Med 2017;9:24.
- Teng A, Nair M, Wells J, Segre JA, Dai X. Strain-dependent perinatal lethality of Ovol1-deficient mice and identification of Ovol2 as a downstream target of Ovol1 in skin epidermis. Biochim Biophys Acta 2007;1772:89–95.
- Theoharides TC, Zhang B, Kempuraj D, Tagen M, Vasiadi M, Angelidou A, et al. IL-33 augments substance P-induced VEGF secretion from human mast cells and is increased in psoriatic skin. Proc Natl Acad Sci USA 2010;107:4448–53.

- Tigelaar RE, Lewis JM, Bergstresser PR. TCR damma/delta+ dendritic epidermal T cells as constituents of skin-associated lymphoid tissue. J Invest Dermatol 1990;94(Suppl. 6):58S-63S.
- Tsuji G, Hashimoto-Hachiya A, Kiyomatsu-Oda M, Takemura M, Ohno F, Ito T, et al. Aryl hydrocarbon receptor activation restores filaggrin expression via OVOL1 in atopic dermatitis. Cell Death Dis 2017;8:e2931.
- Tsuji G, Hashimoto-Hachiya A, Yen VH, Miake S, Takemura M, Mitamura Y, et al. Aryl hydrocarbon receptor activation downregulates IL-33 expression in keratinocytes via Ovo-like 1. J Clin Med 2020;9:891.
- Uribe-Herranz M, Lian LH, Hooper KM, Milora KA, Jensen LE. IL-1R1 signaling facilitates Munro's microabscess formation in psoriasiform imiquimod-induced skin inflammation. J Invest Dermatol 2013;133:1541–9.
- van der Fits L, Mourits S, Voerman JSA, Kant M, Boon L, Laman JD, et al. Imiquimod-induced psoriasis-like skin inflammation in mice is mediated via the IL-23/IL-17 axis. J Immunol 2009;182:5836—45.
- Wood LC, Jackson SM, Elias PM, Grunfeld C, Feingold KR. Cutaneous barrier perturbation stimulates cytokine production in the epidermis of mice. J Clin Invest 1992;90:482–7.
- Zhang X, Yin M, Zhang L. Keratin 6, 16 and 17-critical barrier alarmin molecules skin wounds and psoriasis. Cells 2019;8:807.

#### **SUPPLEMENTARY MATERIALS AND METHODS**

#### Mice

Ovol1+/- mice are maintained in a CD1 strain background (Sun et al. 2021) and are intercrossed to produce homozygous mutant ( $Ovol1^{-/-}$ ) progeny for the study. CD1- $Ovol1^{-}$ mice survive to adulthood but are sometimes smaller than the control littermates, so sex- and weight-matched control and mutant littermates were used for all analysis.

## Imiquimod-induced psoriasis model

Mice aged 7-8 weeks received a daily topical dose of 62.5 mg 5% imiquimod cream (Perrigo, Dublin, Ireland) on shaved backs for 1-5 consecutive days or as indicated. On the basis of a previously described objective scoring system called PASI (van der Fits et al. 2009), erythema (redness of the skin) and scaling (approximated by dry, white cracks and patches on the skin surface) were blindly scored independently by one or more investigators on a score from 0 (none) to 4 (most severe). The cumulative score (erythema plus scaling) served as a measure of the severity of clinical signs (score 0-8).

#### Flow cytometry

To obtain a single-cell suspension, minced samples were digested with 10 ml of a solution containing 0.25% collagenase (C9091, Sigma-Aldrich, St. Louis, MO), 0.01 4-(2-hydroxyethyl)-1-piperazineethanesulfonic (BP310; Thermo Fisher Scientific, Waltham, MA), 0.001 M sodium pyruvate (BP356; Thermo Fisher Scientific), and 0.1 mg/ml DNase (DN25; Sigma-Aldrich) at 37 °C for 1 hour with rotation and then filtered through a 70μm filter, spun down, and resuspended in 2% fetal bovine serum (Alpha FBS; Alphabioregen, Boston, MA). A total of  $5 \times 10^5$  cells were stained by incubation for 30 minutes at room temperature with the following antibodies diluted in 2% fetal bovine serum/×1PBS: Alexa Fluor 488-conjugated anti-CD11b (101217; BioLegend, San Diego, CA), phycoerythrin-conjugated anti-F4/80 (123110; BioLegend), APC-conjugated anti-CD45 (clone 30-F11, 20-0451; Tonbo Biosciences, San Diego, CA), APC-Cy7-conjugated anti-Ly6G (clone 1A8, 25-1276; Tonbo Biosciences), and 7-aminoactinomycin D (559925; BD, Franklin Lakes, NJ).

### Histology and immunostaining

Sections from paraformaldehyde-fixed, paraffin-embedded back skin were stained with H&E, and epidermal thickness was measured at over 30 positions per section, and values were averaged.

For indirect immunofluorescence, mouse back skins were freshly frozen in optimum cutting temperature compound (Tissue-Tek) and stained using the appropriate antibodies. The primary antibodies used were keratin 1, keratin 14, and loricrin (rabbit or chicken, 1:1,000; gifts of Julie Segre, National Institutes of Health, Bethesda, MD), Ki-67 (rabbit, clone #D3B5, catalog number 9129; 1:1,000; Cell Signaling Technology, Danvers, MA), and Ly6G (rat, clone 1A8; 1:200; eBioscience, Waltham, MA). The following secondary antibodies were used: FITC-conjugated goat anti-rabbit (FI-1000; 1:1,000; Vector Laboratories, Burlingame, CA), rhodamineconjugated goat anti-chicken (103-295-155; 1:1,000; Jackson ImmunoResearch Laboratories, West Grove, PA), and Alexa Fluor 488-conjugated donkey anti-rat (A-21208; 1:1,000; Thermo Fisher Scientific). Slides were mounted in Antifade medium (Vectashield H-1000; Vector Laboratories).

# RNA extraction and RT-gPCR

Back skin was collected, and epidermis was separated from the dermis after incubation in a 1:1 dilution of dispase in Epilife media (M-EPICF-500; Cascade Biologics, Portland, OR) at 37 °C for 1 hour. The epidermis was then lysed in TRIzol (15596018; Thermo Fisher Scientific), followed by chloroform extraction and RNA purification from the agueous phase using Zymo Research's Quick-RNA MiniPrep per the manufacturer's instructions.

For RT-qPCR, 2 µg of RNA was used to generate cDNA (4368814; Applied Biosystems, Waltham, MA) as per the manufacturer's instructions. qPCR was performed using a Bio-Rad CFX96 Real-Time System and SsoAdvanced Universal SYBR Green Supermix (172-5271; Bio-Rad Laboratories, Hercules, CA). Gapdh was used as a loading control. Information for the gene-specific primers used is provided in Supplementary Table S1.

# OVOL1 knockdown in normal human epidermal keratinocytes and Ovol1 deletion in primary mouse keratinocytes

Normal human epidermal keratinocytes (KCs) were cultured in Keratinocyte SFM (17005042; Gibco, Waltham, MA). OVOL1 small interfering RNA was purchased from Thermo Fisher Scientific (small interfering RNA identification 115544) and transfected into normal human epidermal KCs on six-well plates using Lipofectamine RNAiMAX Transfection Reagent (13778030; Invitrogen, Waltham, MA) according to manufacturer's instructions. One day after transfection, the medium was replaced, and normal human epidermal KCs were treated with calcium ion (1.8 mM) for 24 hours.

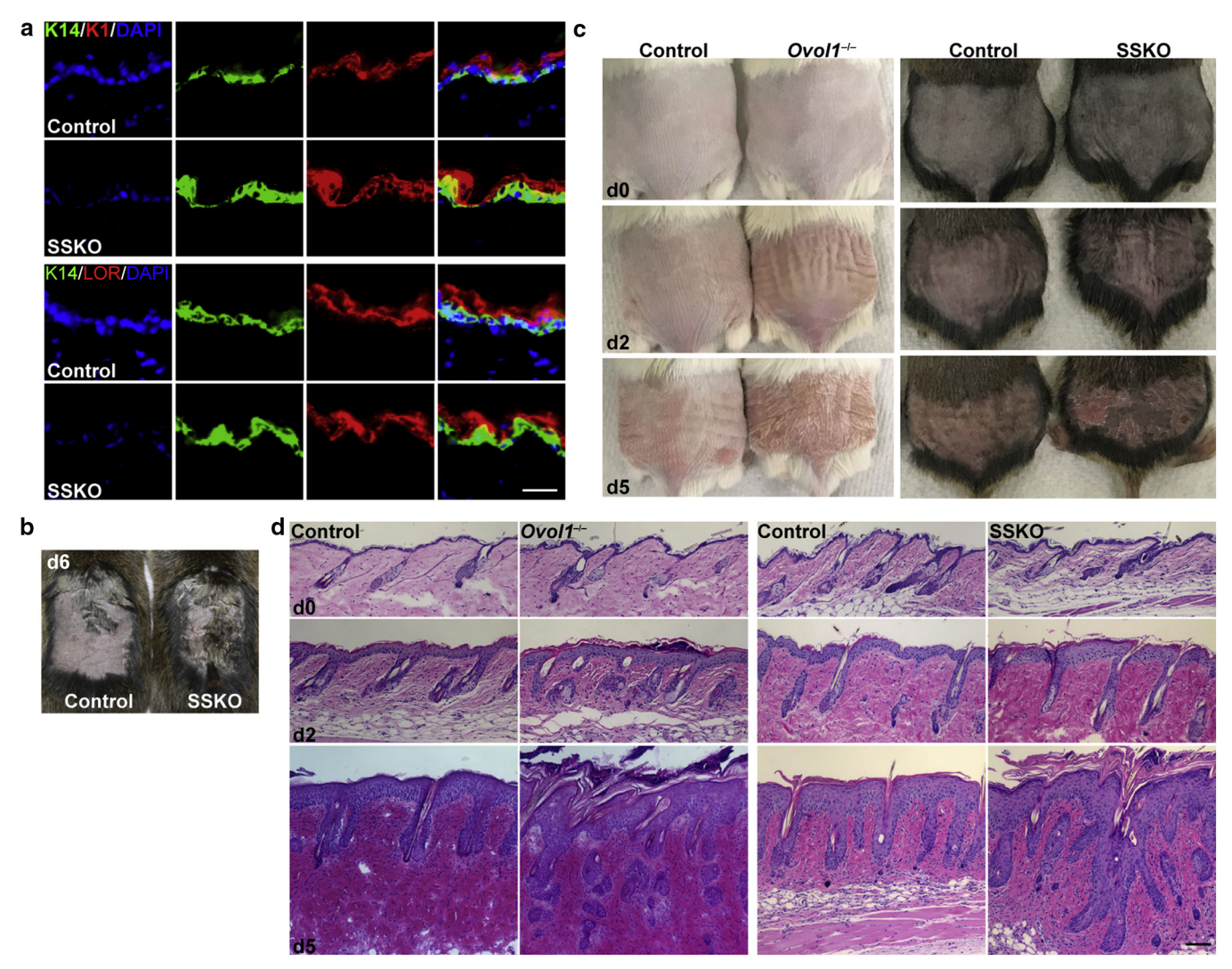
Primary mouse KCs were isolated from newborn Ovol1<sup>f/f</sup> mice as described in the study by Haensel et al. (2019) with minor modification. Briefly, the epidermis was separated from the dermis by overnight incubation with dispase. The epidermis was dissociated on a drop of TrypLE Express Enzyme (12604013; Gibco) for 30 minutes at room temperature. KCs were cultured in Epidermal Keratinocyte Medium (CnT-07, CELLnTEC, Bern, Switzerland). For acute deletion of Ovol1, 50,000 KCs were infected with adenoviruses expressing Cre recombinase (multiplicity of infection = 100) or control adenoviruses, centrifuged at 500g at room temperature for 2 hours, followed by incubation for 24 hours on 12-well plates. KCs were treated with calcium ion (1.8 mM) in a fresh medium for 24 or 48 hours.

#### **SUPPLEMENTARY REFERENCES**

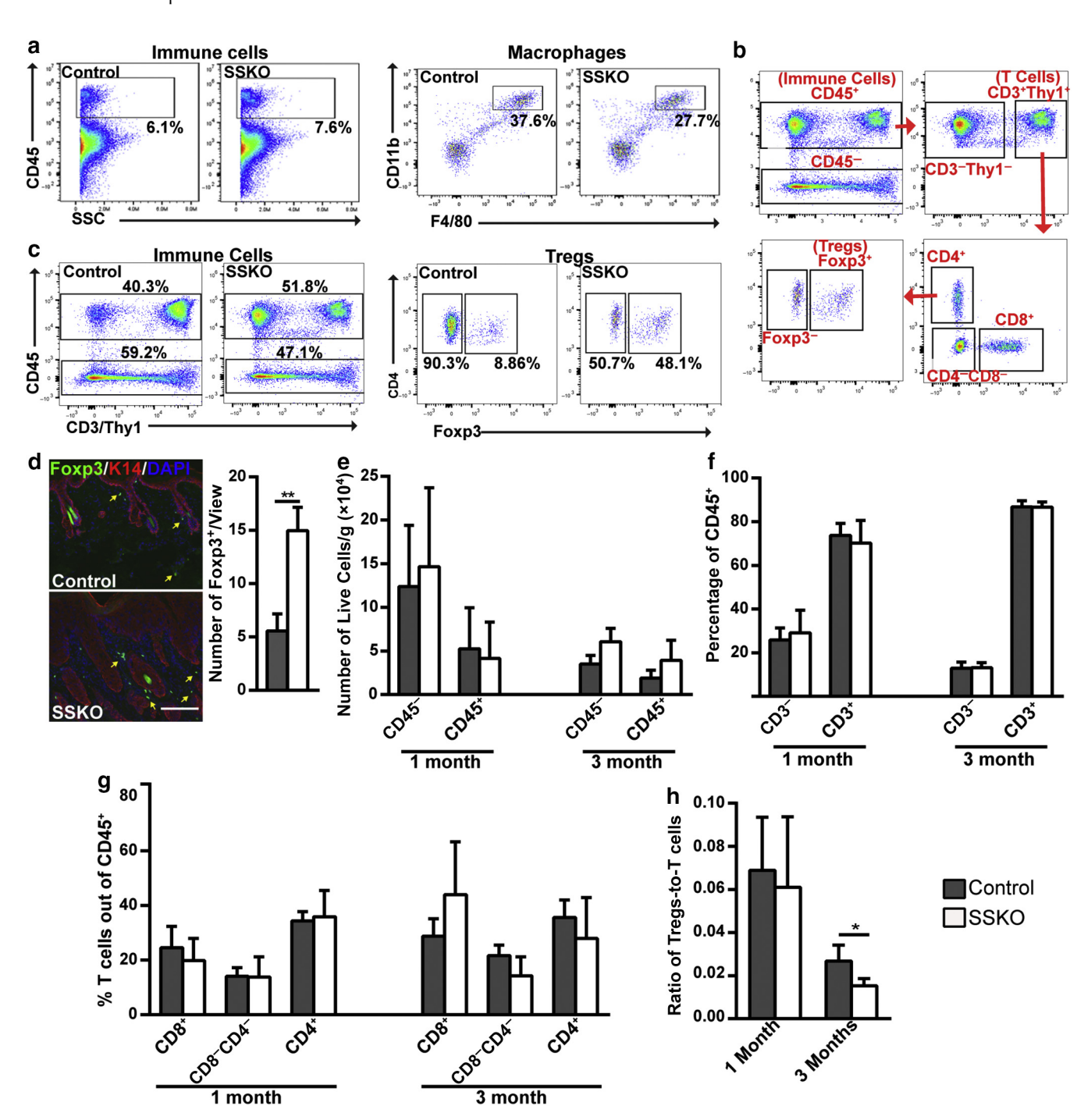
Haensel D, Sun P, MacLean AL, Ma X, Zhou Y, Stemmler MP, et al. An Ovol2-Zeb1 transcriptional circuit regulates epithelial directional migration and proliferation. EMBO reports 2019;20:e46273.

Sun P, Vu R, Dragan M, Haensel D, Gutierrez G, Nguyen Q, et al. OVOL1 regulates psoriasis-like skin inflammation and epidermal hyperplasia. J Invest Dermatol 2021;141:1542-52.

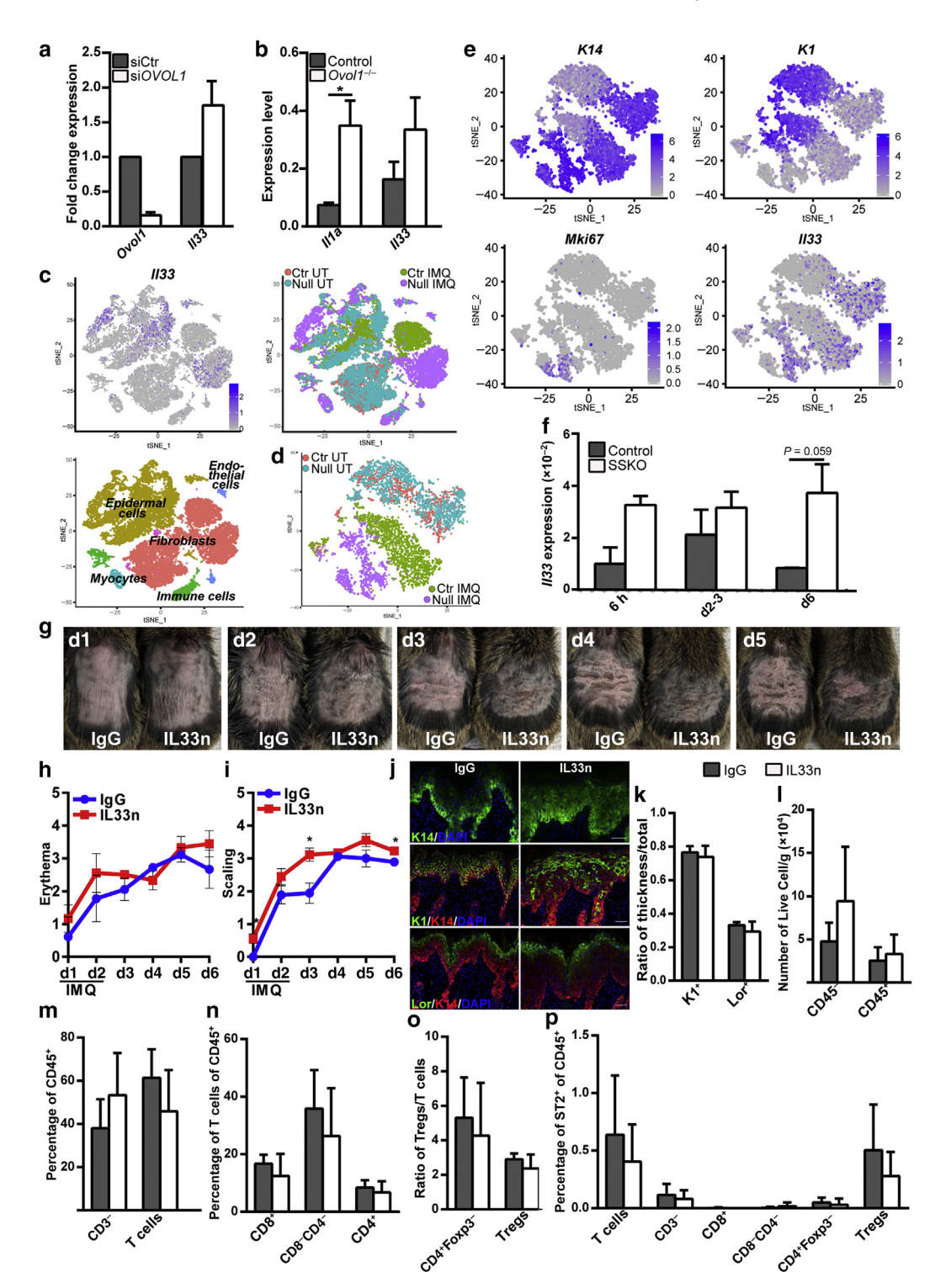
van der Fits L, Mourits S, Voerman JSA, Kant M, Boon L, Laman JD, et al. Imiguimod-induced psoriasis-like skin inflammation in mice is mediated via the IL-23/IL-17 axis. J Immunol 2009;182:5836-45.



Supplementary Figure S1. Ovol1 SSKO mice show exacerbated epidermal hyperplasia after only two IMQ applications. This figure is related to Figure 1. (a) Representative immunofluorescent staining of untreated Ovol1 SSKO and littermate control back skin. Bar = 15 µm. (b) Representative images of Ovol1 SSKO mice and control littermates 6d after two IMQ applications. (c) External appearance and (d) histology of the skin of Ovol1<sup>-/-</sup> (left) and Ovol1 SSKO (right) mice and their respective control littermates at the indicated times after five IMQ treatments. Bar =  $100 \, \mu m$ . d, day; IMQ, imiquimod; K, keratin; LOR, loricrin; SSKO, skin epithelia-specific knockout.



Supplementary Figure S2. Flow plots and immune cell profiles in control and *Ovol1* SSKO skin 1–3 months after IMQ treatment. This figure is related to Figure 2. (a) Representative flow cytometry plots for Figure 2a. (b) Gating strategy for Figure 2b—e. (c) Representative flow cytometry plots for Figure 2c and d. (d) Representative immunofluorescent staining and quantification of Foxp3<sup>+</sup> Tregs in the skin 6 days after two IMQ applications. Arrows point to Tregs. (e—h) Summary of flow cytometry data for the respective immune cell populations 1–3 months after two IMQ applications. n = 7 controls at 1 month and 6 controls at 3 months; n = 6 and 3 for *Ovol1* SSKO mice for 1 and 3 months, respectively. \*\* P < 0.01; \* P < 0.05. IMQ, imiquimod; K, keratin; SSC, side scatter; SSKO, skin epithelia—specific knockout; Treg, regulatory T cell.



Supplementary Figure S3. Supplementary data on the expression and function of Il33 in Ovol1-deficient skin. This figure is related to Figure 3. (a) RT-qPCR analysis on siCtr and siOvol1-treated NHEK cells. Results from a single experiment are shown but are representative of three independent experiments. (b) RTqPCR analysis 6 h after IMQ treatment in  $Ovol1^{-/-}$  mice. n = 5 for  $Ovol1^{-/-}$  and 4 for control littermates. (c) Feature plot showing the expression of Il33 in all cell types detected in the single-cell analysis of mouse 24 h after IMQ treatment. tSNE plots from Sun et al. (2021) depicting the samples (center) and cell (right) types are included for comparison. Ctr-UT and Ctr-IMQ represent untreated and IMQ-treated control littermate (Ovol1+/-) skin, respectively. Null-UT and Null-IMQ represent untreated and IMQ-treated Ovol7<sup>-/-</sup> skin, respectively. (d, e) Single-cell data on interfollicular epidermal cells. Shown are (d) tSNE and (e) genespecific feature plots. (f) RT-qPCR analysis on whole skin of control and Ovol1 SSKO mice at the respective times after two IMQ applications. n = 2 pairs of Ovol1 SSKO and controls for 6 h, n = 4 pairs of Ovol1 SSKO and controls for 2-3 d, and n = 3 pairs of Ovol1 SSKO and controls for 6 d. (g) External appearance, (h) erythema, or (i) scaling scoring at the indicated times. (j) Representative immunofluorescent staining of the indicated markers on d6. (k) The relative thickness of the K1- or LOR-positive layers relative to the total combined epidermal thickness was calculated and shown in i. (I-p) Flow cytometry on d6 for the indicated cell populations. n=3 pairs of IgG-treated and IL33n-treated Ovol1 SSKO mice. \*P < 0.05. (a, b, e, g, h, j, o) Error bars represent the mean  $\pm$ SD. Ctr, control; d, day; h, hour; IMQ, imiquimod; K, keratin; LOR, loricrin; NHEK, normal human epidermal keratinocyte; siCtr, control small interfering RNA; siRNA, small interfering RNA; SSKO, skin epithelia-specific knockout; Treg, regulatory T cell; tSNE, t-distributed stochastic neighbor embedding; UT, untreated.

Supplementary Figure S4. Supplementary data on neutrophil depletion experiments. This image is related to Figure 5. (a) Skin histology of Ovol1<sup>-/-</sup> mice treated with IgG or Ly6G antibody on d3. (b, c) Analysis of (b) epidermal thickness and (c) cell proliferation in Ovol1<sup>-/-</sup> mice treated with IgG or Ly6G antibody at the experimental endpoint. n = 3 for Ovol1<sup>-/-</sup> and 1 for wild-type control littermate. Error bars represent the mean  $\pm$  SEM. (**d**) External appearance on different d before and after IMQ treatment. Note that these mice are distinct from those shown in Figure 5. Ab, antobody; d, day; IMQ, imiquimod.

